Explaining the Enhanced Photocatalytic Activity of Degussa P25 Mixed-Phase TiO_2 Using EPR

Deanna C. Hurum, Alexander G. Agrios, and Kimberly A. Gray*

Institute for Environmental Catalysis and Department of Civil Engineering, Northwestern University, Evanston, Illinois 60208

Tijana Rajh and Marion C. Thurnauer*

Chemistry Division, Argonne National Laboratory, Argonne, Illinois 60439

Received: November 5, 2002; In Final Form: February 11, 2003

Charge separation characteristics of a high-activity, mixed-phase titania photocatalyst (Degussa P25) are probed by EPR spectroscopy. While previous proposals consider rutile as a passive electron sink hindering recombination in anatase, this research details the critical and active role of rutile in TiO_2 formulations. The inactivity of pure-phase rutile is due in part to rapid rates of recombination. Yet, in mixed-phase TiO_2, charges produced on rutile by visible light are stabilized through electron transfer to lower energy anatase lattice trapping sites. These results suggest that within mixed-phase titania (P25) there is a morphology of nanoclusters containing atypically small rutile crystallites interwoven with anatase crystallites. The transition points between these two phases allow for rapid electron transfer from rutile to anatase. Thus, rutile acts as an antenna to extend the photoactivity into visible wavelengths and the structural arrangement of the similarly sized TiO_2 crystallites creates catalytic "hot spots" at the rutile−anatase interface.

Introduction

Semiconductor photocatalysis is widely studied as the technological basis for solar energy storage cells,[1−4] catalytic synthesis of organic compounds,[5] and the degradation of organic contaminants in both gas phase and aqueous systems.[6,7] Much of this work is focused on titanium dioxide due to its low cost, ready commercial availability, stability in water, and band energies that are well matched to the redox properties of water.[8,9] Yet, given the wide range of photoefficiencies observed among various TiO_2 phases and formulations, past research has been unable to explain comprehensively the high photoactivity observed in some mixed-phase TiO_2 preparations such as Degussa P25.

The two principal catalytic phases of TiO_2, anatase and rutile, have numerous structural and functional differences. Commercially available anatase is typically less than 50 nm in size. These particles have a band gap of 3.2 eV, corresponding to a UV wavelength of 385 nm. The adsorptive affinity of anatase for organic compounds is higher than that of rutile,[10] and anatase exhibits lower rates of recombination in comparison to rutile due to its 10-fold greater rate of hole trapping.[11] In contrast, though some exceptions exist, the thermodynamically stable rutile phase generally exists as particles larger than 200 nm.[12] Rutile has a smaller band gap of 3.0 eV with excitation wavelengths that extend into the visible at 410 nm. Nevertheless, anatase is generally regarded as the more photochemically active phase of titania, presumably due to the combined effect of lower rates of recombination and higher surface adsorptive capacity.

The development of TiO_2 materials for use as paint pigments has serendipitously led to titania catalysts with enhanced photoactivities. While some of these mixed-phase materials have limited use as pigments, such formulations of TiO_2 exhibit higher photocatalytic activity than either pure phase alone.[13] Due to the higher activity of pure-phase anatase compared to rutile, anatase is conventionally considered to be the active component in mixed-phase catalysts, with rutile serving passively as an electron sink. These mixed-phase TiO_2 formulations have been used in many innovative commercial applications for the control of organic contamination including air-purifying bathroom tiles and self-cleaning glass surfaces for the consumer market.[14−16] Commercial opportunities such as these emerge when TiO_2 materials are developed that show slower rates of recombination, exhibit increased photoefficiencies, and are activated by lower energy light. To develop catalysts with these desired properties, characterization methods, such as electron paramagnetic resonance spectroscopy (EPR), are useful in probing the fundamental nature of the enhanced photoactivity.

The utility of a semiconductor photocatalyst such as TiO_2 lies in its ability to convert photons into chemical energy. The absorption of ultra-band gap energy promotes an electron from the valance band to the conduction band, leaving a positively charged hole in the valence band. Most of the charge pairs recombine either radiatively or nonradiatively, accounting in part for low photoefficiency and differences in the photoactivity of various catalysts. A small fraction of the electrons and holes move to the surface and either react by direct electron transfer with an adsorbed compound or migrate into trapping sites prior to either surface reaction or recombination.

Originally proposed in the early 1990s, the current hypothesis of the enhanced activity of mixed phases relative to pure phases is that the transfer of electrons from anatase to a lower energy rutile electron trapping site in mixed-phase TiO_2 catalysts serves to reduce the recombination rate of anatase, leading to more

* Corresponding authors. E-mail: k-gray@northwestern.edu; MarionT@anl.gov.

10.1021/jp0273934 CCC: $25.00
Published on Web 04/19/2003

efficient electron−hole separation and greater catalytic reactivity.[17] The data supporting this hypothesis, however, are ambiguous and the phenomenon has not been fully investigated. While the model has gained support on the basis of the lower energy conduction bands of rutile relative to anatase, these arguments do not take into consideration the energies of the lattice or surface trapping sites, which can be significantly lower. For example, the anatase trapping site has been shown to be 0.8 eV lower in energy than the anatase conduction band, placing it below the rutile conduction band as well.[18] Recent reports have also suggested the possibility of electron "spillover" from rutile in high-temperature treated materials.[19]

In this work, P25 (Degussa:Hulls), as a model of high-activity, mixed-phase TiO_2 photocatalysts, is studied using EPR. Typically, the activity of different catalyst formulations is evaluated empirically by testing the material using small model compounds such as 2-propanol, ethylene, or chloroform to quantify and compare photooxidation.[20,21] EPR, however, is well suited to probe on a molecular level the dynamics of charge separation, and therefore photocatalytic behavior, in TiO_2 both directly[22] and by spin trapping methods.[11,23]

When a semiconductor such as TiO_2 is illuminated at 4 K, as is common in low-temperature EPR experiments, there is generally not enough energy for diffusion of the photogenerated charges from trapping sites. The hole rapidly migrates to the surface trapping sites while electrons are initially observed primarily in Ti(III) lattice trapping sites. The rapid appearance of the holes at the surface is explained by self-trapping of photogenerated electrons in the particle interior lattice.[24,25] Furthermore, the structural geometry of rutile and anatase are sufficiently different that paramagnetic properties of trapped electrons in the two phases are distinct and can be resolved using EPR.[26] While the low temperature of the EPR experiment does change the kinetics of transfer to and from these trapping sites, it does not affect the pathway of charge transfer.

Charge separation in several aggregate size samples of P25 was monitored by investigating the fate of photoproduced charged pairs and their trapping sites in order to explain behavior in different TiO_2 catalyst compositions. With EPR, subsequent migration of the electron/hole pairs was examined by measuring the changes in local symmetry and spin−lattice interactions. These measurements provide detailed molecular information about charge-transfer behavior among the titania phases, thereby explaining features that contribute to the enhanced activity of a mixed-phase catalyst.

Materials and Methods

Degussa P25 was kindly donated by Degussa:Hulls Corporation. Colloidal samples of Degussa P25 of various size were prepared by sonication of an aqueous slurry of P25 for 1 hour, followed by centrifugation in Sorvall rotor SA-600 at 4500 rpm for 45 min. Using Stoke's law, the size of the particles collected was estimated and confirmed by filtering collected colloid through prewashed syringe filters (Pall-Gelman) of appropriate pore size. After separation, the aqueous samples were concentrated by slow evaporation under a nitrogen flow. Both sonicated and unsonicated suspended slurry samples of P25 were studied and no difference was detected between the two treatments.

Distilled deionized water was used with a resistivity of 18 MΩ/cm. HPLC grade methanol (E-M Science) was used without further purification. Titania suspensions for EPR experiments were degassed by nitrogen purge. The anatase used for comparison to the Degussa P25 samples was prepared by methods previously discussed[26] since commercially available pure-phase anatase frequently contains paramagnetic centers of unknown origin that interfere with spectral interpretation.

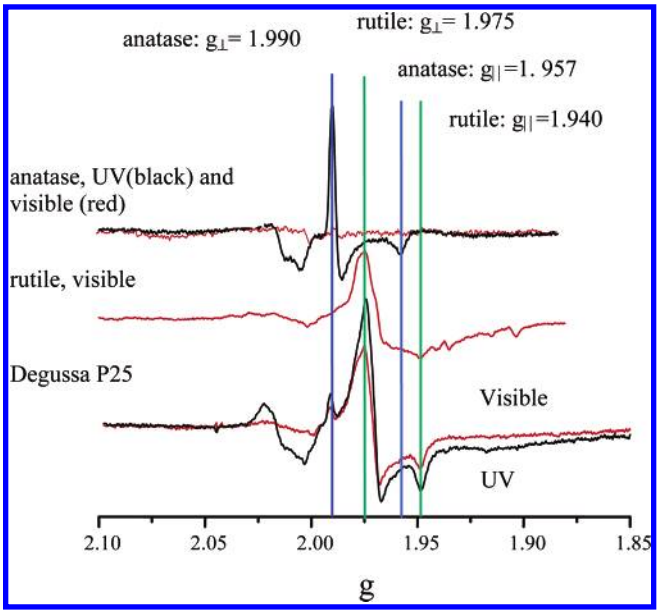

Figure 1. EPR spectra of a P25 aqueous slurry under visible (marked in red) and UV illumination, in comparison to those of rutile and anatase under UV and visible (marked in red) illumination. Note the absence of any anatase signal under the experimental visible illumination conditions.

EPR spectra were collected on a Varian E-9 spectrometer equipped with a helium cryostat. Samples were cooled to 10 K and illuminated within the cavity at that temperature while spectra were acquired. A 300 W xenon lamp (ILC Inc.) was used. Initial illumination typically lasted for a duration of 30 min. For visible light experiments, the lamp was filtered by a Schott 400 nm long pass filter. Control experiments with pure-phase anatase were performed to check for band-gap excitation under the experimental conditions. No charge separation was observed in the anatase samples.

To study charge separation and recombination, the samples were monitored at two additional temperatures after irradiation, 80 and 120 K. The samples were warmed in the dark to the higher temperature, and then cooled to 10 K in order to regain sensitivity. In this way, charge separation and transfer could be tracked. Prior to illumination, samples were monitored for any dark background signals, as was the microwave cavity both before and after illumination.

Results and Discussion

Upon illumination of an aqueous P25 slurry with visible light (>400 nm) at 10 K, the EPR spectrum shown in red in Figure 1 is observed. In this spectrum there are two major features: signals from holes and signals from electrons. A broad signal at $g = 2.014$ is assigned to surface hole trapping sites. In this work the hole signals are not sufficiently resolved to confirm whether the hole trapping site is an anatase oxygen site, a rutile oxygen site, or some combination of the two. The sharp signal at $g_\perp = 1.990$ and shoulder at $g_{||} = 1.957$ are assigned to lattice electron trapping sites in anatase. The remaining signals at $g_\perp = 1.975$ and $g_{||} = 1.940$ are the lattice electron trapping sites in rutile. The parallel components of the spectra are much weaker than the perpendicular components and are easily obscured. The spectra observed agree well with those measured for pure-phase samples as shown in Figure 1 and with literature values independently found for Ti(III) centers in anatase and rutile.[22,27,28]

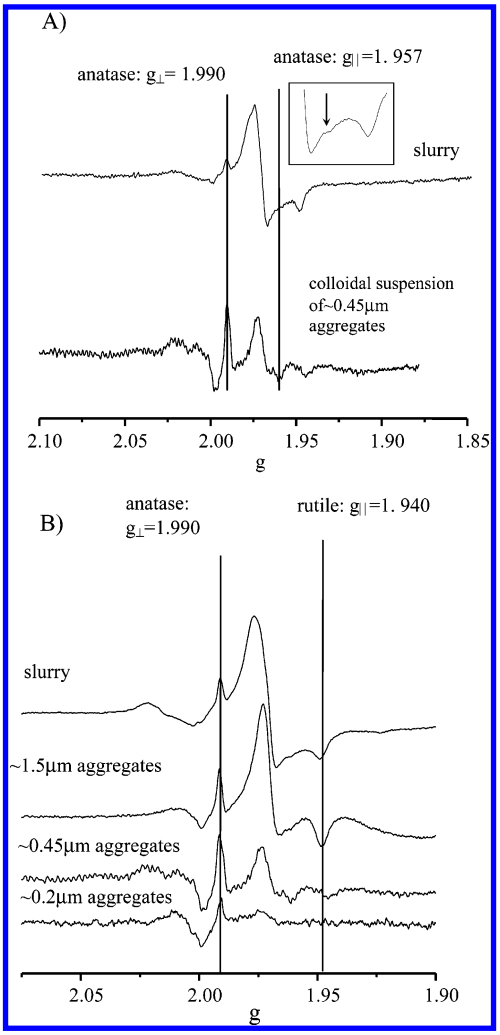

Figure 2. (A) EPR spectra of a P25 colloidal suspension and an aqueous slurry. The slurry sample has broader spectral lines and a weaker anatase signal, as marked. The parallel component of the anatase signal is enlarged in the boxed inset. (B) Spectra of size-fractionated P25 suspensions. Note the decrease in the anatase signal as particle size increases. Representative features of the anatase and rutile spectra are marked for comparison. A background cavity signal has been subtracted from these spectra.

It is important to note the presence of the Ti(III) signal characteristic of an anatase environment in the P25 sample under visible illumination conditions. Under identical conditions with pure-phase anatase no signal and therefore no charge separation was observed. Irradiation of the Degussa P25 sample with the full output of the UV lamp yields the spectrum of the same Ti(III) electron trapping sites with a slight increase in the overall signal intensity. The weak signal composed of three lines at $g = 2.007$, $g = 2.014$, and $g = 2.024$ are resonances from the oxygen-centered surface hole trapping sites. The anisotropy of this signal is indicative of the low symmetry of the surface sites. The nature of the surface trapping sites has been thoroughly studied in previous work on pure-phase anatase.[26]

In addition to the P25 slurry samples, colloidal suspensions of P25 were studied. These samples also exhibited signals characteristic of both anatase and rutile. Figure 2A compares the spectra of an unsonicated 45 mg/mL P25 slurry and a colloidal suspension under visible illumination. While both anatase and rutile lattice trapping sites are populated in each sample, there are significant differences between the two spectra. The more prominent appearance of the anatase lattice trapping site spectral features in the colloidal suspension is due to both a decrease in the spectroscopic line width and an increase of the anatase signal intensity relative to that of rutile. In the slurry sample the spectra are broadened as a result of variable aggregate size.

To further investigate the origins of the anatase lattice trapping signal we prepared a series of P25 colloidal suspensions using a modified sonication/centrifugation method.[29] Figure 2B shows the spectra for colloidal P25 suspensions illuminated by visible light. The smallest colloidal suspension is composed of ~0.2 μm (200 nm) aggregates composed of clusters of anatase and rutile crystallites. The 200 nm size of these small aggregates indicates that the rutile phases present within them are smaller than those generated by typical synthetic methods.[12] In this spectrum, the anatase signals are clearly observed and a very weak rutile component is present. The weak rutile signal indicates that the vast majority of the lattice trapping sites in this aggregate size range are in anatase. In this size fraction, the electrons generated by charge separation in rutile are readily transferred to anatase. Under the same experimental conditions, no trapping sites were observed in pure-phase anatase.

In the spectrum from a 0.45 μm (450 nm) size fraction as shown in Figure 2B, the rutile signal intensity relative to the anatase signal is larger than in the 0.20 μm colloid, indicating that the proportion of rutile to anatase in the larger aggregate is greater than that of the smaller aggregate. The spectrum from aggregates of approximately 1.5 μm (1500 nm) shows a much stronger rutile signal and a weak anatase signal, although it is larger than the same anatase signal in the mixed slurry sample. Thus, as the aggregates increase in size, EPR results show that the population of rutile lattice trapping sites increases. In other words, as the aggregate size increases the trapped charges remain on rutile and less transfer to anatase occurs.

These results demonstrate that within P25 there is an inhomogeneous mixture containing variable aggregate sizes in which the proportion of rutile within an aggregate increases as the aggregate size increases. We propose that the observed electron transfer is due to interwoven rutile and anatase crystallites that form tightly bound nanoclusters. The presence of large rutile crystallites in the 1.5 μm clusters and aggregates of clusters cause electrons generated by visible light at 10 K to remain trapped on rutile, resulting in a more intense rutile EPR signal which masks the observation of electron transfer from rutile to anatase. At 10 K, charges can only be transferred between chemically bonded clusters. Interparticle, or intercluster, charge-transfer cannot occur. The EPR results indicate that aggregates in P25 are composed of variable-sized rutile/anatase clusters. Small aggregate sizes (<200 nm) require that the rutile crystallites are atypically small, on the same order of magnitude as the anatase. As the cluster size decreases, the surface-to-bulk ratio increases, whereby anatase predominates over the rutile fraction and we observe electron transfer from rutile to anatase. Therefore we suggest that the smaller, high-activity clusters within an aggregate are mixed-phase having a core of rutile crystallites interwoven with bound anatase crystallites, maximizing the transfer of electrons from rutile to neighboring anatase sites. This structural arrangement is consistent with HR-TEM data collected by us and others.[30] Working with the sonicated and centrifuged colloid allows for the selection of a controlled composition of the catalyst. In our experiments, we selected aggregates that are in the 0.45 μm range to remove the effects from large clusters dominated by rutile and to study the electron-transfer properties between TiO_2 phases.

The spectrum in Figure 3a shows an illuminated (λ > 400 nm) P25 colloid at 10 K. The hole trapping sites and the two

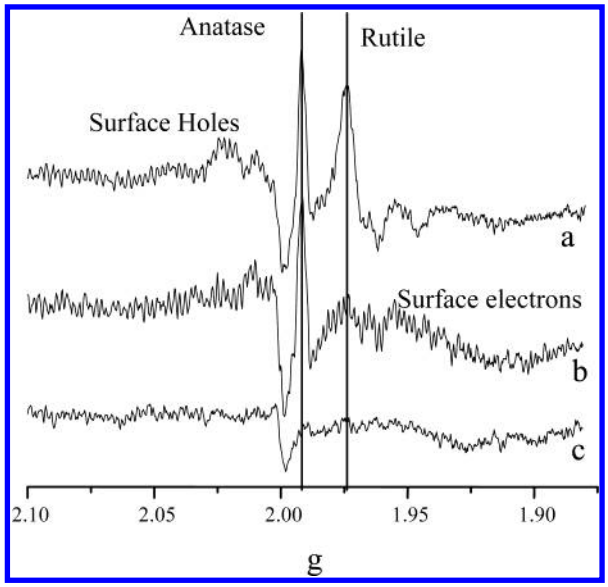

Figure 3. Degussa P25 colloid (a) under visible illumination, (b) after 80 K annealing, and (c) after 200 K annealing.

electron trapping sites are both observed. The anatase signal was not present in control samples of pure-phase anatase under the same conditions. To investigate electron migration, the P25 sample was warmed to allow for electron transfer and then returned to 10 K for data acquisition. The spectra are displayed normalized to the hole trapping signal to correct for charge recombination at the elevated temperature. Upon warming to 80 K (Figure 3b), the rutile signal vanishes, and an increased anatase signal accumulates. Additionally, a broad signal characteristic of an anatase surface electron trapping site emerges.[26,31] Since there is no additional illumination, the anatase electron trapping site can only be populated by electron transfer from the rutile to the anatase. Further warming to 200 K allows for recombination of the trapped anatase electrons and the trapped surface electrons with surface holes, leaving only a cavity background signal.

To confirm the source of the anatase signal and rule out recombination rate differences, holes were scavenged from the photoexcited catalyst to prolong the lifetime of the photogenerated electrons. Methanol efficiently scavenges holes from the surface, as in the half reaction below:

$$CH_3OH + Ti(IV){-}O^{\bullet +} \rightarrow {}^{\bullet}CH_2OH + Ti(IV){-}O + H^+ \qquad (+1.2V)$$

This process competes with recombination and in this work is used to isolate the electron-transfer processes from recombination.[31,32]

Upon initial visible illumination of the P25 colloids in the presence of methanol at 10 K, the spectrum shown in Figure 4A is observed. This figure shows that, after addition of methanol, a spectrum characteristic of methanol radicals on the TiO_2 surface ($g = 2.004$, $A = 18$ G) was observed.[33] The third line of the methanol radical triplet is obscured by the anatase signal.[31] The signals from the electron traps again demonstrate that both anatase and rutile trap centers are populated.

When the illumination is stopped, immediate charge transfer is observed. Figure 4B shows the change in the intensity of the signals from the three trapping sites observed as a function of time after illumination at constant temperature (10 K). These data have not been corrected for recombination and represent a direct measure of the change in the signal intensity. As can be

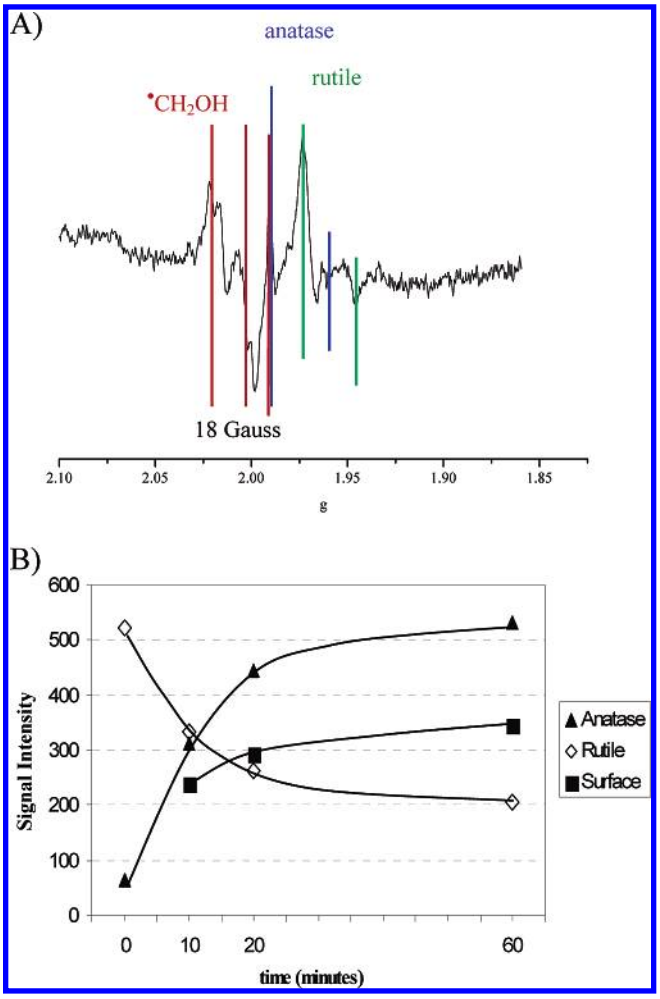

Figure 4. (A) Initial spectrum of Degussa P25 colloid under visible illumination. Marked lines show the spectrum of methanol radicals with a characteristic 18 G hyperfine splitting. Anatase and rutile signals are also visible. The third line of the methanol radical triplet is overlapped with the anatase signal. (1.0 mW microwave power, $T = 15$ K, UV illumination.) (B) Electron transfer in colloid after illumination. As the number of rutile trapping sites decreases, the anatase and surface site signal intensities (arbitrary units) both increase. As a result of low signal intensity, measurement of surface trapping sites during illumination ($t = 0$) was not possible. Lines serve as guides for the eye only.

seen, the anatase trapping sites and surface trapping sites each increase in intensity, and therefore population, while the rutile trapping sites decrease. This direct evidence confirms the transfer of rutile electrons to anatase. This electron-transfer reaction has an estimated activation barrier of less than 8.3×10^{-4} eV based on the measured rate of transfer.[34] In order for such a low activation energy for electron transfer to be possible, the sites must be in very close contact. HR-TEM experiments on the dry powder indicate that Degussa P25 consists of clustered individual crystallites of anatase and rutile, with rutile being slightly larger on average.[11,30] These rutile particles are much smaller than typical for pure-phase rutile. Our spectroscopic data are consistent with the HR-TEM data and indicate that unusually small rutile crystallites must be interwoven with anatase crystallites to facilitate the efficient electron transfer at the anatase/rutile interface creating catalytic "hot spots." Such "hot spots" have been previously observed on anatase phase titania aggregates by atomic force microscopy.[35] Additionally, work by Banfield and co-workers indicates highly distorted regions at anatase crystal interfaces which have been identified as rutile nucleation sites.[36] Such sites would be entirely

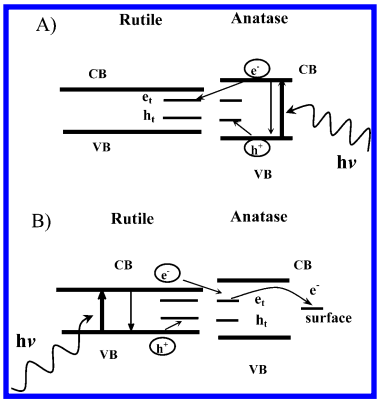

Figure 5. (A) Previously speculated model of P25 activity where charge separation occurs on anatase and rutile acts as an electron sink. (B) Proposed model of a rutile antenna and subsequent charge separation.

consistent with the data we observe and facilitate rapid electron transfer between the phases.

The efficiency of most photocatalysts is determined to a large degree by recombination rates. Despite the fact that the photoactivity of rutile extends into the visible light range, pure-phase rutile is photocatalytically inactive. It has been established that rutile exhibits high rates of recombination in comparison to anatase.[11,37] Yet, when charge recombination is inhibited by a sensitizing dye, rutile performs as effectively as anatase.[38] Our work illustrates that the proximity of anatase to rutile serves to scavenge rutile electrons and stabilize the charge separation, preventing rapid recombination. We attribute the high catalytic activity of mixed-phase TiO_2 catalysts in large part to this synergistic activation of the rutile phase by anatase. The rutile phase extends the photoactive range into the visible, harvesting more light, and electron transfer from rutile to anatase trapping sites hinders charge recombination.

Conclusions

According to the traditional model, the increased activity of Degussa P25 is due to a rutile sink, preventing anatase recombination and allowing an anatase-originating hole to move to the surface (Figure 5A). The data we have gathered do not support this model. By the current models, the rutile centers would be more populated after temperature annealing or after allowing time for electron transfer. Instead we observe the opposite, an increase in the anatase centers. Rutile is more integral to the activity of the catalyst than a simple electron sink for anatase. The presence of small rutile crystallites creates a structure where rapid electron transfer from rutile to lower energy anatase lattice trapping sites under visible illumination leads to a more stable charge separation. Transfer of the photogenerated electron to anatase lattice trapping sites allows holes that would have been lost to recombination to reach the surface. Subsequent electron-transfer moves the electron from anatase trapping sites to surface trapping sites, further separating the electron/hole pair (Figure 5B). By competing with recombination, the stabilization of charge separation activates the catalyst and the rutile-originating hole can participate in oxidative chemistry.

From the data we have gathered, mixed-phase titania catalysts show greater photoeffectiveness due to three factors: (1) the smaller band gap of rutile extends the useful range of photoactivity into the visible region; (2) the stabilization of charge separation by electron transfer from rutile to anatase slows recombination; (3) the small size of the rutile crystallites facilitates this transfer, making catalytic hot spots at the rutile/anatase interface. This process depends critically on the interface between the TiO_2 phases and particle size. The atypically small size of the rutile particles in this formulation, and the intimate contact with anatase that the comparable size allows, are crucial to enhancing the catalyst activity.

Acknowledgment. The authors thank Degussa:Hulls for their generous donation of P25. The authors also thank Prof. Laurence Marks and Natasha Erdman for HR-TEM discussions and assistance. This work was supported by the Northwestern University Institute for Environmental Catalysis (IEC), funded through a grant from the National Science Foundation (NSF) with matching funds from Northwestern University and the U.S. Department of Energy (CHE-9810378). IEC work at Argonne National Laboratory supported by the U.S. Department of Energy, Office of Basic Energy Sciences, Division of Chemical Sciences, under contract W-31-109-Eng-38.

References and Notes

(1) Bach, U., et al. *Nature* **1998**, *395*, 583.
(2) Hagfeldt, A.; Grätzel, M. *Acc. Chem. Res.* **2000**, *33*, 269.
(3) Serpone, N. *Res. Chem. Intermed.* **1994**, *20*, 953.
(4) Lewis, N. S. *Am. Sci.* **1995**, *83*, 534.
(5) Fox, M.; Dulay, M. T. *Chem. Rev.* **1993**, *93*, 341.
(6) Chiron, W.; Fernandes-Alba, A.; Rodriguez, A.; Garcia-Calvo, E. *Water Res.* **2000**, *34*, 366.
(7) Anderson, M. A. *Stud. Surf. Sci. Catal*. **1997**, *103*, 445.
(8) Linsebigler, A. L.; Lu, G.; Yates, J. T. *Chem. Rev.* **1995**, *95*, 735.
(9) Hoffmann, M. R.; Martin, S. T.; Choi, W.; Bahnemann, D. W. *Chem. Rev.* **1995**, *95*, 69.
(10) Stafford, U.; Gray, K. A.; Kamat, P. V.; Varma, A. *Chem. Phys. Lett.* **1993**, *205*, 55.
(11) Riegel, G.; Bolton, J. R. *J. Phys. Chem.* **1995**, *99*, 4215.
(12) Yin, H., et al. *J. Mater. Chem.* **2001**, *11*, 1694.
(13) Bacsa, R. P.; Kiwi, J. *Appl. Catal. B* **1998**, *16*, 19.
(14) Wang, R., et al. *Nature* **1997**, *388*, 431.
(15) Asahi, R., et al. *Science* **2001**, *293*, 269.
(16) Tryk, D. A.; Fujishima, A.; Honda, K. *Electrochem. Acta* **2000**, *45*, 2363.
(17) Bickley, R. I., et al. *J. Solid State Chem.* **1991**, *92*, 178.
(18) Leytner, S.; Hupp, J. T. *Chem. Phys. Lett.* **2000**, *330*, 231.
(19) Emeline, A., et al. *J. Photochem. Photobiol. A* **2002**, *148*, 97.
(20) Choi, W.; Termin, A.; Hoffmann, M. R. *J. Phys. Chem.* **1994**, *98*, 13669.
(21) Yamazaki, S.; Fujinaga, N.; Araki, K. *Appl. Catal. A* **2001**, *201*, 97.
(22) Howe, R.; Gratzel, M. *J. Phys. Chem.* **1985**, *89*, 4495.
(23) Liu G., et al. *Environ. Sci. Technol.* **1999**, *33*, 2081.
(24) Rajh, T., et al. *Chem. Phys. Lett.*, **2001**, *5*, 31.
(25) Asahi, R., et al. *Phys. Rev. B* **2000**, *61*, 7459.
(26) Micic O., et al. *J. Phys. Chem.* **1993**, *97*, 7277.
(27) Meriaubeau, P. *Chem. Phys. Lett.* **1970**, *5*, 131.
(28) Kerssen, J.; Volger, J. *Physica* **1973**, *69*, 535.
(29) Sun, L.; Bolton, J. R. *J. Phys. Chem.* **1996**, *100*, 4127.
(30) Datye, A. K., et al. *J. Solid State Chem.* **1995**, *115*, 236.
(31) Rajh, T., et al. *J. Phys. Chem.* **1996**, *100*, 4538.
(32) Micic, O., et al. *J. Phys. Chem.* **1993**, *97*, 13284.
(33) Sullivan, P. J.; Koski, W. S. *J. Am. Chem. Soc.* **1963**, *85*, 384.
(34) Atkins, P. W. *Physical Chemistry, 5th ed.*; W. H. Freeman and Company: New York, 1994; pp 877−878.
(35) Farneth, W. E., et al. *Langmuir* **1999**, *25*, 8569.
(36) Penn, R. L.; Banfield, J. F. *Am. Mineral.* **1999**, *84*, 871.
(37) Sclafani, A.; Herrmann, J. M. *J. Phys. Chem.* **1996**, *100*, 13655.
(38) Park, N.; van de Lagemaat, J.; Frank, A. *J. Phys. Chem. B* **2000**, *104*, 8989.